Brain correlates of phonological recoding of visual symbols

Sylvain Madec, Kévin Le Goff, Jean-Luc Anton, Marieke Longcamp, Jean-Luc Velay, Bruno Nazarian, Muriel Roth, Pierre Courrieu, Jonathan Grainger, Arnaud Rey

BRAIN CORRELATES OF PHONOLOGICAL RECODING OF VISUAL SYMBOLS

Sylvain Madec[1,4*], Kévin Le Goff[1,4], Jean-Luc Anton[2,4], Marieke Longcamp[3,4],

Jean-Luc Velay[3,4], Bruno Nazarian[2,4], Muriel Roth[2,4],

Pierre Courrieu[1,4], Jonathan Grainger[1,4] and Arnaud Rey[1,4]

1. Laboratoire de Psychologie Cognitive – CNRS
Aix-Marseille University, Marseille, France

2. Centre IRM Fonctionnelle, Institut des Neurosciences de la Timone – CNRS
Aix-Marseille University, Marseille, France

3. Laboratoire de Neurobiologie de la Cognition – CNRS
Aix-Marseille University, Marseille, France

4. Brain and Language Research Institute,
Aix-Marseille University, Marseille, France

Running Head: PHONOLOGICAL RECODING

* Corresponding author:

Arnaud Rey
Laboratoire de Psychologie Cognitive – CNRS
Université Aix-Marseille
3, place Victor Hugo - Case D
13331 Marseille Cedex 03 – France
E-mail: arnaud.rey@univ-amu.fr

Abstract

Learning to read involves setting up associations between meaningless visual inputs (V) and their phonological representations (P). Here, we recorded the brain signals (ERPs and fMRI) associated with phonological recoding (i.e., V-P conversion processes) in an artificial learning situation in which participants had to learn the associations between 24 unknown visual symbols (Japanese Katakana characters) and 24 arbitrary monosyllabic names. During the learning phase on Day 1, the strength of V-P associations was manipulated by varying the proportion of correct and erroneous associations displayed during a two-alternative forced choice task. Recording event related potentials (ERPs) during the learning phase allowed us to track changes in the processing of these visual symbols as a function of the strength of V-P associations. We found that, at the end of the learning phase, ERPs were linearly affected by the strength of V-P associations in a time-window starting around 200 ms post-stimulus onset on right occipital sites and ending around 345 ms on left occipital sites. On Day 2, participants had to perform a matching task during an fMRI session and the strength of these V-P associations was again used as a probe for identifying brain regions related to phonological recoding. Crucially, we found that the left fusiform gyrus was gradually affected by the strength of V-P associations suggesting that this region is involved in the brain network supporting phonological recoding processes.

Introduction

Several studies have explored the physiological basis of reading by using functional magnetic resonance imaging (fMRI) and have emphasized the contribution of a brain region located on the left ventral occipitotemporal cortex (left vOT), sometimes designated as the "visual word form area" (VWFA, see Cohen et al., 2000; McCandliss, Cohen, & Dehaene, 2003). These studies have reported invariance of this region's activity to case and letter fonts (Dehaene et al., 2001; Dehaene, Le Clec'H, Poline, Le Bihan, & Cohen, 2002), invariance to the spatial location of the stimuli (Cohen et al., 2002), differential activities for letters and their mirror images (Pegado, Nakamura, Cohen, & Dehaene, 2011), and similar functional properties for this region across various cultures and writing systems (Bolger, Perfetti, & Schneider, 2005; Liu et al., 2008). On the basis of these results, it has been suggested that the VWFA would code for abstract representations involved in orthographic processing (Polk & Farah, 2002; for a review, see Dehaene & Cohen, 2011).

This proposition is consistent with general properties of the ventral visual system. It has indeed been proposed that the anterior part of left VOT would code for visual information that is invariant to low-level visual factors and that, from posterior to anterior regions, it would be organized hierarchically with neural detectors coding for increasingly larger receptive fields and tuned to increasingly complex and abstract representations (for reviews, see Logothetis & Sheinberg, 1996; Grill-Spector & Malach, 2004; Rolls, 2000). Within a neurobiological model assuming a central role of the VWFA (i.e., the local combination detector model, Dehaene et al., 2005) it has been suggested that word recognition would be organized in sequential computational steps that would be activated in a purely feed-forward fashion and that would depend on neural detectors hierarchically organized along the visual stream. In this framework, non-orthographic representations (i.e., phonological or semantic) would not be triggered as long as orthographic processing would not be completed. Therefore,

none of these higher-level representations would contribute to orthographic processing (Simos et al., 2002; for a discussion, see Carreiras, Armstrong, Perea, & Frost, 2014).

However, the functional role of left vOT (or VWFA) is still actively debated (e.g., Dehaene & Cohen, 2011; Price & Devlin, 2011). First, specificity of left vOT to orthographic processing is contested by studies showing that left vOT is equally activated by pictures of objects and by words (Sevastianov et al., 2002; Wright et al. 2008; Vogel, Petersen, & Schlaggar, 2012; Kherif, Josse, & Price, 2011). Second, meta-analyses have shown that several other language-related brain regions localized in the left hemisphere are also activated during reading (Turkeltaub, Eden, Jones, & Zeffiro, 2002; Jobard, Crivello, & Tzourio-Mazoyer, 2003; Vigneau et al., 2006). These regions include the temporo-parietal cortex, including inferior parietal and superior temporal regions, as well as the inferior frontal cortex. Concerning the inferior parietal regions, the supramarginal gyrus (SMG) has been associated with phonological processing (Church, Balota, Petersen, & Schlagaar, 2011; Stoeckel, Gough, Watkins, & Devlin, 2009; Price, Moore, Humphreys, & Wise, 1997; Wilson, Tregellas, Slason, Pasko, & Rojas, 2011) while the angular gyrus (AG) has been associated with semantic processing (Price et al., 1997). Concerning the superior temporal regions, the superior temporal gyrus (STG) has also been associated with phonological processing (Price, Wise, & Frackowiak, 1996; Rumsey et al.,1997; Simos et al., 2002). The inferior frontal gyrus (IFG), and specifically its opercular part, has been considered as being implicated in articulatory representations (Gitelman, Nobre, Sonty, Parrish, & Mesulam, 2005; Klein et al., 2015; Mainy et al., 2008; Pugh et al., 1996; Sandak et al., 2004). Contributions of these brain regions are consistent with early neurological models of reading (e.g., Ben-Shachar et al., 2007) proposing that visual processing in the occipital cortex is relayed to the AG before converging to the left posterior superior temporal cortex (for a contrasting view concerning AG, see Price, 2000; Price & Mechelli, 2005).

The non-specificity of left vOT to orthographic processing and, moreover, its location within a network embedding visual and language related regions indicate that the activation of left vOT could be modulated by brain regions coding for higher-level representations, especially phonological representations (Price & Devlin, 2003; Price et al., 2011). Indeed, several studies suggest a sensitivity of left vOT to manipulations of task context and higher-order stimulus properties (Cai, Paulignan, Brysbaert, Ibarrola, & Nazir, 2009; Twomey, Duncan, Price, & Devlin, 2011; Woodhead, Brownsett, Dhanjal, Beckmann, & Wise, 2011; Mano et al, 2013; Seghier & Price, 2011; Song, Tian, & Liu, 2012), and that priming effects on left vOT are equally induced by orthographic and non orthographic stimuli (Kherif et al., 2011). These top-down effects could rely on white matter pathways connecting left vOT to other regions such as the left temporal lobe through the inferior longitudinal fasciculus, the left prefrontal cortex through the inferior fronto-occipital fasciculus, and the left vertical occipital fasciculus that projects to the lateral occipital parietal junction, including AG and the left lateral superior occipital lobe (Yeatman, Rauschecker, & Wandell, 2013; Yeatman, Weigner, Pestilli, Rokem, Mezer, & Wandell, 2014; for a review on diffusion tensor and reading, see Vandermosten, Boets, Wouters, & Ghesquière, 2012). Consistent with these results, an alternative neural model of reading has been proposed, (i.e., the *interactive account*, Price & Devlin, 2011; see also Carreiras et al., 2014) in which the activity within left vOT would reflect the integration of *feedforward* information coming from visual inputs and *feedback* information coming from areas involved in higher-level processing (e.g., phonological, semantic).

The literature on visual letters presented in isolation partially mirrors the literature and debates on written word processing. Several studies compared the processing of letters to the processing of different kinds of visual shapes like faces (Tarkiainen, Cornelissen, & Salmelin, 2002; Wong, Jobard, James, James, & Gauthier, 2009), digits (Polk & Farah, 1998), single

geometric shapes (Garrett et al., 2000; Flowers et al., 2004), objects (Joseph, Gathers, & Piper, 2003), or unfamiliar characters (Wong et al., 2009). Overall, these results suggest sensitivity to letters of an area within the left vOT that is slightly more anterior and medial than the VWFA. More recently, Rothlein and Rapp (2014) found that this area was insensitive to letter case and to letter names, while being sensitive to letter identity. The left vOT could therefore be the host of an abstract level of representation for single letters, while being immune to higher-level representations.

However, a series of studies challenged the selective account of this area to letters by applying more rigorous definitions of selectivity. Pernet, Celsis, and Demonet (2005) showed that the left and right vOT were activated in a similar manner by Roman, non-Roman letters and symbols in a discrimination task. The categorization task in the same experiment showed significantly less activation for the Roman letter category within left vOT, as compared with non-Roman letters and symbols. Flowers et al. (2004) showed that a portion of left vOT was only significantly enhanced by attending to the alphabetic properties of letters, and not by attending to low level visual components (i.e., such as the color). Joseph, Cerullo, Farley, Steinmetz, and Mier (2006) partially replicated the results of Pernet et al. (2005) by showing a differential activity within left vOT between letters and other objects, solely appearing in a silent reading task. Taken together, these results suggest that there would be a form of top-down modulation of left vOT by higher-level representations while attending to single letters.

Another set of studies investigated in adults the effect of learning the associations between unknown visual symbols and phonological representations. Callan, Callan, and Masaki (2005) trained participants to learn phonological representations associated to a non-native alphabet. In a two-back identification task on native and non-native alphabets (pre- and post-learning), they failed to find a modulation of the activity of left vOT after training but showed an enhancement of AG activity and an increase in psychophysiological interactions

between AG and STG. In another study, Hashimoto and Sakai (2004) showed that the activity of left vOT and the parieto-occipital cortex is enhanced after learning associations between unfamiliar characters and speech sounds. They also observed an enhancement of the functional connectivity between these areas after learning. However, task-dependent factors might explain the discrepancies between these two learning studies due to variations in the involvement of phonological recoding. Finally, Xue, Chen, Jin, and Dong (2006) used an artificial language training paradigm in which participants were successively familiarized with the visual shape, phonology and semantic of new visual symbols. Results showed a decrease in left vOT activation after visual training, and an increase in left vOT and IFG activations after phonological and semantic training. These studies therefore provide additional evidence on the role of left vOT and related regions in the phonological recoding of visual symbols.

In the present study, we also used an artificial learning paradigm in order to further investigate the role of left vOT and related areas in the development of associations between visual symbols and phonological representations. The originality of our approach is to manipulate parametrically the strength of visuo-phonological (V-P) associations. During the learning phase, four lists of V-P associations were created and the strength of these associations was varied across the four lists by manipulating the proportion of correct and incorrect associations. Our hypothesis was straightforward: by varying the strength of V-P associations, the activation of brain areas involved in phonological recoding should also vary as a function of the strength of the associations.

In addition to studying the brain regions involved in the development of V-P associations, we were also interested in investigating the time-course of phonological recoding during the acquisition of these associations. Studies using methodologies with fine-grained temporal resolution (e.g., MEG or EEG) and single letters as visual symbols have

provided converging evidence about the dynamics and time-course of letter perception processes. MEG and event-related potential (ERP) studies have reported results indicating that low-level visual processing occurs around 100 ms after stimulus onset and that an item-specific activity starts after 150 ms (e.g., Carreiras, Perea, Gil-López, Mallouh, & Salillas, 2013; Rey, Dufau, Massol, & Grainger, 2009; Tarkiainen et al., 2002; Tarkiainen, Helenius, Hansen, Cornelissen, & Salmelin, 1999; Wong, Gauthier, Woroch, DeBuse, & Curran, 2005). Using a masked priming paradigm, Petit, Midgley, Holcomb, and Grainger (2006) found that a later component, designated as P260 (220–300 msec), was sensitive to the name of letters, suggesting that phonological recoding would take place during that time-window (see also Madec, Rey, Dufau, Klein, & Grainger, 2012). A second goal of the present study is therefore to further document the time-window during which phonological representations are accessed and activated by recording ERPs during the learning phase of V-P associations. Finding an early effect of these associations on ERPs would provide additional evidence for top-down influences of phonology on the processing of visual symbols.

In the present study, participants had to learn the associations between 24 unknown visual symbols (Japanese Katakana characters) and 24 arbitrary names. During the learning phase, four groups of 6 V-P associations were created by varying the strength of these associations. This was done by a parametric manipulation of the proportion of correct and erroneous associations displayed in a two-alternative forced choice task that was used during the learning phase. ERPs associated to visual symbols were recorded during that period. The parametric modulation of the strength of these associations was then used as a probe for assessing an effect of phonological recoding on ERPs. One day after the training phase, participants had to perform a final training on V-P associations followed by an fMRI session in which the strength of these associations was again used as a probe for identifying brain regions related to phonological recoding.

Experiment

Participants

Twenty-four participants (14 females), with age ranging from 21 to 36, (mean age = 26.6, σ = 3.6) participated in the experiment. All participants were right-handed native speakers of French with normal or corrected-to-normal vision. None of the participants were familiar with Katakana characters and none of them reported history of psychiatric or neurological disorders. All participants received a financial compensation for their participation. This study received a prior approval from the Ethics Committee of Aix-Marseille University and the CNRS (N° RCB 2010-A00155-34) and all participants signed a written informed consent before starting the experiment.

Overview of the experiment (*Figure 1a*)

The entire experiment was planned on 2 consecutive days. During the first day, in the afternoon, participants learned the associations between 24 Katakana symbols and their corresponding names. After being exposed initially to these 24 V-P associations, participants performed a two-alternatives forced choice (2AFC) task in which, on each trial, a visual symbol was displayed and followed by one of the 24 possible names. Participants simply had to produce a yes-response if the displayed V-P association was correct and a no-response otherwise.

During this learning phase, Katakana symbols were divided into 4 groups corresponding to the 4 learning conditions that were obtained by varying gradually the exposure to correct associations during the 2AFC task. Out of 6 presentations of each visual symbol, the correct association was presented 5 times in the easiest learning condition, and 4, 2, and 1 times in the other learning conditions, respectively. Therefore, in the most difficult learning condition, participants saw the correct association only once out of 6 presentations of the same visual symbol.

During the 2 AFC task, Event-Related Potentials (ERPs) were recorded and epoched to the visual presentation of Katakana symbols in order to track ERP modifications related to the development of these gradual V-P associations. This learning phase was organized in 12 sessions of 92 trials and every two learning sessions, participants had to perform a naming task on the 24 Katakana symbols in order to directly test their acquisition of these V-P associations. There were no ERP recording during the naming task.

During the second day, in the morning, participants started with two learning sessions (identical to the ones done on Day 1) with no ERP recording. They also had to perform one naming task. This initial testing guaranteed that participants correctly learned the V-P associations. Participants were then tested within the MRI and had to perform a matching task.

< insert Figure 1 around here >

Material

Stimuli consisted in 24 Katakana symbols (*Figure 1b*). An arbitrary name corresponding to a Consonant-Vowel syllable was given to each of the 24 symbols. This arbitrary name prevented participants from learning these associations at home between Day 1 and Day 2 (by searching on the web, for example). Two sets of phonemes, 6 consonants and 4 vowels, were used to create each name by combining all the consonants to all the vowels. These phonemes were chosen to generate names that could be easily perceived and produced by native French speakers. These 24 Katakana symbols were divided into 4 groups of 6 symbols corresponding to the 4 learning conditions (i.e., Group 1: /ka/, /la/, /ti/, /bi/, /me/, /re/; Group 2: /ki/, li/, /te/, /be/, /mo/, /ro/; Group 3: /ke/, /le/, /to/, /bo/, /ma/, /ra/; Group 4: /ko/, /lo/, /ta/, /ba/, /mi/, /ri/). We controlled for the influence of low-level visual factors, possibly differing between the 4 groups of Katakana symbols, by associating each of the 24 (*4!*) permutations of the four groups to the 4 learning conditions (L1, L2, L3 and L4). Therefore,

each participant had a unique association between each group of Katakana symbols and each learning condition, and every group of Katakana symbols was associated with every learning condition 6 times on the whole group of participants.

A set of 26 uppercase Roman letters, displayed in the *Inconsolata* font, was used as a behavioral baseline condition in order to compare response times and accuracies for the four learning conditions to the performance on overlearned V-P associations (i.e., letters with their names). Six Roman letters were used in this baseline condition (D, F, L, P, R and V) and the remaining letters were used as fillers.

Sound files corresponding to the names of all stimuli (24 Katakana and 26 alphabetical letters) were recorded by one of the experimenters (AR) and digitized at 44100 Hz in a single channel. Mean durations of the names were 449 ms and 442 ms, for Katakana and letter names respectively (range and standard deviation for Katakana: [357 429] ms and 47 ms; for letters: [322 606] ms and 78 ms).

During the 2AFC and naming tasks, all stimuli were presented on a 17" cathode ray tube (CRT) monitor, with a refresh rate of 60 Hz, as white signs on an 800 x 600 pixels black background (32 x 24 cm). Participants were seated at 80 cm from the screen. These tasks were controlled by a personal computer using E-Prime (Psychology Software Tools, Pittsburgh, PA). During the learning phase and the 2AFC task, all names were presented through in-ears headphones. During the matching task (on Day 2, within the MRI), stimulus presentation and response recording were monitored by a specific software using the National Instruments LabVIEWVR environment and a digital hardware.

Learning phase: 2AFC task, ERP recording and preprocessing

On Day 1, after completing informed consent, participants seated comfortably in a sound-attenuated and dimly lit room. At the beginning of the learning phase, participants were first presented all the 24 V-P associations. During this initial exposure phase, a trial started

with a fixation cross (‘+’) for 200 ms, followed by an empty screen for 500 ms. A Katakana symbol was then presented in the middle of the screen for 700 ms together with its associated name. It was followed by an empty screen of 500 ms. All Katakana symbols were presented at this stage in a random order.

After this initial exposure to the 24 V-P associations, participants had to learn these associations while performing a 2AFC task during which the EEG signal was recorded. In this task, each trial started with a fixation cross ('+') for 200 ms, followed by an empty screen during a randomized duration ranging from 400 to 600 ms (see *Figure 2a*). The visual stimulus (Katakana symbol or alphabetic letter) was then presented in the middle of the screen. After a randomized duration ranging from 500 to 700 ms, an auditory name was orally presented and the visual stimulus remained on the screen until the participant’s response. Response times were recorded from the onset of the auditory name. Feedback was finally provided during 300 ms (green checklist symbol for correct responses and red cross for errors). Each trial ended with an inter-trial interval that consisted in an empty screen for a randomized duration ranging from 400 to 600 ms. Participants were requested to be as accurate and as fast as possible. They were also asked to remain as relaxed as possible in order to avoid movements that could generate artifacts on the EEG recording (e.g., eye blinks during the visual presentation of the stimuli or frowning movements).

< insert Figure 2 around here >

By manipulating the amount of exposure to the correct associations during the 2AFC task, 4 learning conditions were created. The 4 groups of Katakana symbols were assigned to each of these conditions. Out of 6 presentations of each Katakana symbol, the correct V-P association was presented 1, 2, 4 or 5 times in the L1, L2, L3 and L4 learning conditions, respectively. Due to this experimental manipulation, participants had therefore more opportunities to learn the correct association in the L4 condition (by seeing 5 times the correct

association out of 6 trials) and gradually, fewer opportunities in the L3 to L1 conditions (with only one exposure to the correct association, out of 6 trials, in the L1 condition). Alphabetical letters were presented with their correct names on half of the letter trials.

Every symbol from L1, L2, L3, L4 were visually presented 36 times during the learning phase. Therefore, there were 36*6 = 216 trials for each of the four learning conditions and a total of 4*216 = 864 trials involving Katakana symbols. Note that the experiment was constructed so that the name of each of the 24 visual symbols from conditions L1, L2, L3 and L4 also appeared 36 times (i.e., they were used to construct negative response trials).

The learning phase was divided in 12 learning sessions, each composed of 92 trials. Among the 92 trials, there were 18 trials from each learning condition (i.e., 18*4 = 72 trials involving Katakana symbols) and 20 trials involving Roman letters (3 presentations of the 6 letters taken from the baseline condition, and one presentation of two randomly selected filler letters). The first two trials of a session consisted in filler trials (i.e., Roman letters) and were discarded. Trials were presented in a quasi-random order with two constraints: two identical visual stimuli could not be presented successively, and the same constraint applied to the presentation of two identical names. Participants could take a break between each session. During the 2AFC task on Day 2, participants performed two sessions similar to the session on Day 1, but without ERP recording.

In order to track changes in performance during the learning phase in Day 1, we divided this phase in 3 parts. Part 1 corresponded to learning Sessions 1 to 4, Part 2 to learning Sessions 5 to 8, and Part 3 to learning Sessions 9 to 12. For each of these parts, we tested the parametric modulation of performance following a linear contrast defined by the strength of the V-P associations for each learning group (see *Appendix A*).

During the 2AFC task on Day 1, the EEG was recorded from 64 Ag/AgCl Active-2 pre-amplified electrodes (BIOSEMI, Amsterdam; 10–20 system positions). The vertical electro-oculogram (EOG) was recorded by mean of one electrode (Ag/AgCl) just below the right eye. The horizontal EOG was recorded with two electrodes (Ag/AgCl) positioned over the two outer canthi. Analog signal was digitized at 1024 Hz. Electrode offsets were kept below ±25 μV. Offline, data were referenced on the mean of mastoid electrodes. Continuous signals were band-pass filtered by using a *butterworth* filter of order 4 between 0.02Hz and 40 Hz. The resulting signals were then epoched between -300 and 1000 ms before and after the presentation of the visual symbol. We relied on an independent components analysis (Makeig, Bell, Jung, & Sejnowski, 1996), as implemented in the *runica* EEGLAB function (Delorme & Makeig, 2004; Delorme, Sejnowski, & Makeig, 2007), to identify artefactual ocular components related to blink activities. They were identified and removed by visual inspection of their scalp topographies, time-courses and activity spectra. Subsequently, we re-epoched signals between -100 and 500 ms before and after the presentation of the visual symbol, and subtracted the average baseline between -100 and 0 ms from each time-point, electrode-by-electrode. We excluded all trials with abnormal activities after a trial-by-trial visual inspection. Finally, a Laplacian transformation (Perrin, Pernier, Bertrand, & Echallier, 1989; as implemented by Cohen, 2014) was applied to the epoched signal (maximum degree of Legendre polynomial: 10, order of splines: 4, smoothing parameter = 10^{-5}). Thereby we obtained ERPs evoked by the presentation of visual symbols for each of the learning conditions L1, L2, L3 and L4.

As for the behavioral results, ERPs at the individual level were analyzed by estimating the linear contrast with weights [-2 -1 1 2] associated to L1, L2, L3 and L4 (see *Appendix A*). At the group level, we computed a one-sample t-test through a bootstrap t-approach, by relying on the LIMO toolbox (Pernet, Chauveau, Gaspard, & Rousselet, 2011), for every pair

(*e, t*) defined in the spatial (e) and temporal (t) dimensions. We corrected for multiple comparisons by relying on spatio-temporal clustering (2D clustering; for additional information see Pernet et al., 2011; Maris & Oostenveld, 2007).

Naming task

After having completed two learning sessions (i.e., 2AFC tasks), participants had to perform a naming task involving the 24 Katakana symbols presented in a random order. Participants were instructed to name the symbol as accurately and rapidly as possible. If they could not remember the symbol's name, they were asked to remain silent until the next trial. A trial started with a fixation cross ('+') for 200 ms, followed by an empty screen for 500 ms (see *Figure 2b*). A visual symbol was then presented in the middle of the screen and remained until response or 1000 ms. An empty screen was then presented for 500 ms. Participant's vocal response was completely digitized at 22040 Hz on a single channel in order to check for response accuracies and to determine RTs offline. Given that there were 12 learning sessions, participants had to perform the naming task 6 times. No feedback was provided during the naming task.

In order to estimate RTs for vocal responses in the naming task, we employed a semi-automatic procedure by applying an algorithm based on Teager-Kaiser operator on digitized responses, which detect sudden variations of energy in the acoustic signal (Li, Zhou, & Aruin, 2007). We then visually checked the detected onsets and manually corrected them when needed. Response accuracy was determined by listening to every vocal response. Trials with no answer were considered as errors. No trials were rejected from this analysis. As for the 2 AFC task, in order to track changes in performance during the learning phase in Day 1, we divided it in 3 parts. Part 1 corresponded to naming blocks occurring after learning Sessions 2 and 4, Part 2 to naming blocks occurring after learning Sessions 6 and 8, and Part 3 to naming

blocks occurring after learning Sessions 10 and 12. Statistical analyses (RTs and ACCs) relied on the same procedure as the one used for the 2AFC task.

Matching task, fMRI acquisitions and preprocessing

During the fMRI recording, participants had to perform a matching task. A block design was used for the fMRI recording that was composed of 4 experimental runs during which functional images were collected. Each run was composed of 30 blocks, with 6 blocks for each condition (L1, L2, L3, L4 and Roman letters). The duration of a run was around 8 min.

During a block, a sequence of 5 visual symbols all belonging to a given condition (L1, L2, L3, L4 or letters) were successively displayed during 200 ms (see *Figure 2c*) with an empty screen presented for 2000 ms between items. At the end of this sequence, an empty screen was displayed for a duration ranging from 2000 to 2450 ms, followed by a visual symbol surrounded by a white square (i.e., the target). Participants were instructed to press a button located under their right forefinger if the target was present among the previous 5 visual symbols; they were instructed to press a button located under their right middle finger otherwise. The target always belonged to the same condition as the 5 previously displayed symbols. During an experimental run and for each learning condition (i.e., L1, L2, L3, and L4), 3 blocks corresponded to a yes-response (target present), and 3 blocks corresponded to a no-response (target absent). Since there were only 3 blocks corresponding to a "yes" response (target present) and 6 symbols per condition, we controlled that each symbol was used the same number of times as a target over the 4 runs. Therefore, each symbol was used 2 times as a target during the whole procedure. Since there were only 5 slots for the position of the target within the sequence of 5 symbols, and 12 target-present blocks, we quasi randomized its position over the entire experiment. Therefore, in each condition, the target occupied each of

the 5 slots at least two times (10 blocks). For the 2 remaining blocks, the slot of the target was randomized between slots 2, 3 and 4. No feedback was provided during the matching task.

Before entering the MRI scanner, participants were trained to the matching task using only letter stimuli and for 4 experimental blocks. After training, participants entered the MRI body scanner and performed the 4 functional runs. At the end of the session, a whole brain anatomical MRI data was acquired.

Functional and anatomical data were collected on a 3-Telsa MRI body scanner (Bruker, Medspec, Germany) using a 2-channel head coil. Participants laid in supine position on the scanner bed, with foam padding applied between the participant's head and the coil, to help constrain head movement. Stimuli were projected centrally at the back of the magnet bore, and participants viewed the projected stimuli through a head-coil mounted mirror placed in front of their eyes.

For functional neuroimaging, functional slices acquisition was axial oblique, angled −20° relative to AC-PC plane in order to cover the whole brain. Functional T2*-weighted images were acquired using a gradient echo-planar imaging sequence, with 36 sequential slices of 3 mm-thick/0 mm-gap (repetition time = 2400 ms, echo time = 30 ms, flip angle = 81.6 °, field of view = 192 mm, 64×64 matrix of 3×3×3 mm voxels). Whole brain anatomical MRI data was acquired using high-resolution structural T1-weighted image (MPRAGE sequence, resolution 1×1×1 mm) in the sagittal plane after the functional runs. Prior to the functional runs, a fieldmap acquisition (3D FLASH sequence inter-echo time 4.552 ms) was collected in order to estimate the B0 inhomogeneity and correct the spatial distortions of functional volumes.

Concerning fMRI pre-processing, four dummy scans in each run were discarded in order to ensure that the longitudinal relaxation time equilibration was achieved. Data was pre-processed and analyzed using SPM8 (Wellcome Department of Cognitive Neurology,

London, UK). First, processing consisted in including the voxel displacement map computed using the fieldmap toolbox during the realign and unwarp procedure for distortion and motion correction. Second, the high-resolution structural T1-weighted image was coregistered to the mean EPI image. Third, all MRI volumes were processed with SPM8's New Segment option to generate grey matter (GM) and white matter (WM) images of the participants. Fourth, a DARTEL template was generated and (affine-only) spatial normalized to MNI space. Fifth, that DARTEL template was used to normalize functional data for each participant. Last, each participant's normalized functional data was spatially smoothed using a 6 mm full-width at half isotropic Gaussian kernel.

At the individual level, 12 regressors (one for each experimental condition: L1, L2, L3, L4, letters and target; one for each parameter of head movement: translations in x, y and z and rotations about x (pitch), y (roll) and z (yaw)) were modeled. The experimental blocks were modeled using boxcar functions convolved with the canonical hemodynamic response function (HRF). As for the behavioral and ERP results, regressors associated to L1, L2, L3 and L4 were analyzed by estimating the linear parametric contrast with weights [-2 -1 1 2]. These linear combinations were then integrated at the group levels through inferential analyses which employed non-parametric permutation methods through FSL's *randomize* function (Nichols & Holmes, 2002). A one-sample *t*-test was performed on the individual linear combinations by using the threshold-free cluster enhancement (TFCE) method, which detects clusters of contiguous voxels without setting an arbitrary statistical cut-off and which controls for the family-wise error (FWE) rate at $p < .05$ (Smith & Nichols, 2009). In order to constructs TFCE distribution under H0, 50000 permutations were computed. We then used the FWE corrected 1-*p* maps from the *randomize* function to mask raw *t*-score maps (a similar statistical method was recently employed in Orr & Banich, 2014). Statistical analyses of

behavioral results (RTs and ACCs) of the matching task relied on the same procedure than the one used for the 2AFC and naming tasks.

Results

Behavioral results

Learning task: 2AFC

Results are given in *Table 1*. Reported p-values indicate the probability that a t-value obtained by bootstrap under H0 is above or below the observed t-value. As shown in *Table 1*, all statistical tests were significant at $p < .05$. These results indicate that RTs and accuracies in the 2AFC task were gradually and linearly affected by our learning manipulation involving a gradual strengthening of the V-P associations. These effects appeared rapidly (i.e., they are already present in Part 1 of the learning phase), and are still present on Day 2. *Figure 3* reports mean reaction times and accuracies at the group level for each experimental condition and also for letters (taken as a behavioral baseline).

< insert Table 1 and Figure 3 around here >

Naming task

Table 2 provides the statistical results and *Figure 3* displays mean RTs and accuracy for each condition at the group level.

< insert Table 2 around here >

As shown in *Table 2*, all statistical tests were significant at $p < .05$. Again, both RTs and response accuracy were gradually and linearly affected by our learning manipulation involving the gradual strengthening of V-P associations. This effect also appeared rapidly (as reflected by the results in Part 1), and was still present on Day 2.

ERPs results

Three participants were excluded from the ERP analysis for excessive artifact on the recorded signals. The average number of trials for the remaining participants was 826 (range

[575-986]). Additional details on the number of trials per condition and part of the procedure can be found in *Appendix B*. *Figure 4a* shows the results of this analysis for every electrode and time point (from -100 ms to 500 ms), and every part of the learning procedure (first two rows). None of the electrode and time points showed an effect of the learning condition before Part 3 of the learning phase. The first electrode to display a significant linear effect was P8 at 200 ms, followed by a cluster of electrodes (P8, P10, PO4, PO8) located on right occipital sites between 200 and 345 ms. Another cluster of electrodes showing significant linear effects appeared on left occipital sites between 300 and 345 ms. As an illustration of the emergence of these linear effects (bottom of *Figure 4b)*, we plotted the mean EEG signal evoked by each condition at the P8 electrode (L1, L2, L3 and L4). Significant linear effect can be seen in shaded area in Part 3. Moreover, *Figure 4c* shows the mean of the linear contrast ($\acute{L}_{ERP}$) at the group level and its associated confidence intervals (95%).

< insert Figure 4 around here >

fMRI results

After acquisition, three participants (different from the ones excluded from the ERP analysis) were excluded from further analysis: two were excluded on the basis of their low accuracy in the fMRI task (i.e., 0.61 and 0.46, respectively, while the group mean was 0.89, σ = 0.12; chance level at 0.5) and a third participant was excluded due to technical problems during the fMRI recording.

There was no linear effect on RTs, t(20) = 0.54, p = 0.6 (CI at 95% = [-131; 229]), and no linear effect on ACCs, t(20) = -1.26, p = 0.2 (CI at 95% = [-0.15; 0.03]). We also checked for differences on RTs and ACCs between the 4 learning conditions using one-way analyses of variance and we found no effect of learning conditions on RTs (F(3,80) = 0.3, p = 0.81) or on ACCs (F(3, 80) = 1.61, p = 0.2), indicating that participants did perform the matching task at similar levels for every learning condition.

Maximum intensity projection of significant t-values is given in *Figure 5*, and was created using the scikit-learn package (Pedregosa et al., 2011). Detailed quantitative descriptions of the significant clusters are given in *Table 3*. Five clusters emerged from the TFCE procedure. Cluster #1 was located on the left fusiform gyrus (peak location: [-33, -42, 18], t(20) = 5.21; 31 voxels). Cluster #2 was located in the left temporal lobe in a location corresponding to STG (peak location [-54, -30, 18], t(20) = 5.01; 69 voxels). Cluster #3 was located in the left supplementary motor area (left SMA; peak location [-6, -9, 54]; t(20) = 6.01; 33 voxels). Cluster #4 was located on the left medial frontal gyrus (peak location : [-6, 63, -18]; t(20) = 4.71; 55 voxels). Cluster #5 was located in the left and right posterior cingulate cortices (peak location: [6, -63, 15]; t(20) = 4.40; 54 voxels). *Figure 6* provides slice views of the three first clusters, arranged spatially and centered on the location of their maximal t-values, together with a descriptive representation of the mean magnetic resonance (MR) signals extracted from these clusters (by learning condition, mean linear contrasts and associated 95% CIs).

< insert Figure 6, Figure 5 and Table 3 around here >

Discussion

In this study, we gradually manipulated the strength of visuo-phonological (V-P) associations that participants had to learn and we used this gradual V-P knowledge as a probe to assess the parametric modulation of cerebral activities through ERP and fMRI recordings. Three main results were obtained. First, at a behavioral level, we found that our experimental manipulation was successful since response times and accuracies were monotonically affected by the strength of V-P associations, both in the 2-AFC and in the naming tasks. Second, during the acquisition of V-P associations in the 2-AFC task, we found that ERPs were also affected by the strength of these associations in the last part of the experiment, with significant effects emerging on right occipital sites between 200 and 345 ms post-stimulus

onset and on left occipital sites between 300 and 345 ms. Finally, during the matching task in the fMRI experiment, we found that five brain regions were affected by the strength of V-P associations: the left fusiform gyrus (left vOT), the left temporal lobe (including STG), the left supplementary motor area (left SMA), the left medial frontal gyrus, and the left and right posterior cingulate cortices.

Behavioral results

The results from the 2-AFC and the naming tasks showed that our experimental manipulation indeed allowed us to create four levels of V-P associations. By controlling the number of times correct associations were presented to participants during the 2-AFC task, we were able to create arbitrary V-P associations varying gradually in their strength. In the 2-AFC and naming tasks, this graded effect appeared both on RTs and accuracies, and it was present from the first part of the experiment until the last experimental session, on Day 2. Overall, performance in the four experimental conditions increased progressively during the experiment but never reached the performance obtained on Roman letters. Although accuracy on Day 2 was almost as good in the L4 condition (i.e., the strongest V-P associations) as for Roman letters, RTs in the naming task were still much slower for the learned associations and were still on average greater than 1 second. This indicates that participants would likely need more training in order to reach the same level of performance as obtained for over-learned associations like familiar letters. Crucially, however, the fact that graded performance was obtained as a function of V-P association strength indicates that our manipulation was successful and can therefore be used as a probe for tracking the time-course of phonological recoding in ERPs and the underlying neural generators revealed in the MRI signal.

ERPs results

ERPs were recorded during the 2-AFC task and we found a significant linear relationship between ERPs and the strength of V-P associations during the last part of the

experiment. This linear effect emerged on right occipital sites around 200 ms post-stimulus onset and on left occipital sites around 300 ms. This finding is consistent with previous studies on letter perception indicating that phonological recoding starts on average around 220 ms post-stimulus onset and lasts until response selection at around 300 ms (Petit et al., 2006; Madec et al., 2012; Madec et al., submitted).

One can note, however, that the onset of the linear effect appears on right occipital sites at around 200 ms (occurring slightly later than the N170 component, see *Figure 3b*). Since we applied a Laplacian filter on the data, which improved spatial resolution for the collected ERPs (e.g., Nunez & Srinivasan, 2006; Cohen, 2014), the generators of this linear effect are likely localized in the right hemisphere. This right lateralization does not seem consistent with a straightforward interpretation related to phonological recoding, given that structures supporting phonological processing have been previously localized in the left hemisphere (e.g., Vigneau et al., 2006).

Interestingly, this result can be related to ERPs studies reporting lateralization of the N170 component depending on reading expertise (i.e., Maurer, Brem, Buscher, & Brandeis, 2005; Yum, Holcomb, & Grainger, 2011). For example, Maurer et al. (2005) found a right occipito-temporal N170 component differing between words and symbol strings, but only for children with a high knowledge about letters. On the contrary, Yum et al. (2011) reported that the same contrast on adult participants revealed a N170 effect localized on left occipito-temporal sites. The right lateralized effect in children was interpreted as a precursor of literacy linked to visual familiarity with print. This right lateralization of the N170 effect would then be present at the early stages of the acquisition of V-P associations and would reflect a predominance of visual processing. The left lateralization would come later during learning and would be associated with the maturation and stabilization of phonological recoding. Moreover, in pre-literate children, the N170 has been proposed as a potential biomarker that

could predict later reading ability, with a positive correlation between the N170 amplitude over the right hemisphere at preschool age and the number of words read two years later (Brem et al., 2013).

In a later study, Maurer, Blau, Yoncheva, and McCandliss (2010) trained adult participants to associate symbol-word pairs (i.e., ortho-phonological associations) and compared ERPs pre- and post-training in the context of a one-back task. They observed a pre-/post-training difference on the N170 emerging solely on right occipital sites that was interpreted in terms of visual familiarity with the novel learned symbols. The combination of the one-back task, which does not necessarily require phonological recoding, along with the short training duration could indeed limit the access to phonological representations and enhance visual processing.

In two other studies (Yoncheva, Blau, Maurer, & McCandliss, 2010; Yoncheva, Wise, & McCandliss, 2015), adults had to learn new visual symbols and their names in the context of a reading verification task (by matching these visual symbols to their auditory representations, which requires greater phonological recoding than a one-back task). These studies reported that the laterality of the N170 effect depended on learning instructions. Participants who had to associate holistically these symbols to phonological representations (as in a logographic language, see Mei et al., 2013) displayed a larger N170 component on right occipital sites, while participants who had to associate parts of these symbols to phonemes (like grapheme-to-phoneme associations in alphabetic languages, see also Mei et al., 2013) displayed a larger N170 component on left occipital sites. These results suggest greater recruitment of left-lateralized networks would occur when processing is directed toward grapheme-to-phoneme mapping.

Similarly, Stevens, McIlraith, Rusk, Niermeyer, and Waller (2013) tested participants in a one-back task with letters and pseudo-letters. They found a larger N170 in the left

hemisphere for letters (relative to pseudo-letters) when participants tended to retrieve letter names and a larger N170 in the right hemisphere when participants tended to perform the one-back task on a visual basis. This result suggests that lateralization of the N170 for single letters varied according to the degree of phonological retrieval.

Taken together, these variations in the lateralization of the N170 could account for the right hemisphere localization of the present linear effect of V-P associations. Indeed, instead of considering that the effect starting around 200 ms is directly due to the strengths of V-P associations, the right lateralization of this effect could be interpreted as a side effect of phonological recoding. Because phonological recoding is still weak for some of these associations, participants would have to allocate more resources to visual processing in order to compensate for the weaker V-P associations. The fact that mean naming times were twice as long for Katakana symbols relative to Roman letters also indicates that phonological recoding was not yet automatized.

Our results thereby complement the findings of Maurer et al. (2010) and Yoncheva et al. (2010; 2015). Consistent with Maurer et al. (2010), we found differential activities on right occipital sites after learning to associate visual symbols to their names. In line with Yoncheva et al. (2010; 2015), this right hemisphere activity could be interpreted as a by-product of weak V-P associations that would lead to greater visual processing. The later linear effect obtained around 300-330 ms on left occipital sites would more likely reflect phonological recoding processes that would be delayed in time relative to overlearned symbols such as Roman letters.

fMRI results

In the fMRI experiment, the main result concerns the activation of the left fusiform region that varied linearly with the strength of V-P associations (see *Figure 5*). Its location, in left vOT at MNI coordinates (-33, -42, -18) is slightly more medial than the reported locations

of the VWFA (e.g., Cohen et al., 2002) but is consistent with the results of several fMRI studies on isolated letters (e.g., James & Gauthier, 2006; Rothlein & Rapp, 2014)[1]. This observed sensitivity to the strength of V-P associations suggests that this area is not only affected by purely visual factors but also by higher-level representations involving phonology (Price & Devlin, 2011; see also Carreiras et al., 2014). This result is also consistent with several other studies reporting an effect of phonological processing on activity in the left fusiform gyrus (e.g., Pugh et al., 1996; Hagoort et al., 1999; Paulesu et al., 2000; Levy et al., 2008). It indicates that activity within the left fusiform gyrus could benefit from top-down influences coming from regions involving phonological representations (Price & Devlin, 2011).

Note that this particular pattern of BOLD responses that increase with the strength of V-P associations might be enhanced by the matching task used in the present experiment. Indeed, Mano et al. (2013) recently showed that left vOT responses associated to words and pseudowords, as compared to consonants strings, were enhanced, but only in the context of an overt naming task and not in a nonlinguistic visual task (for a similar account on single letters, see also Flowers et al., 2004). These task dependent variations might explain previous inconsistent findings obtained in studies using a similar experimental learning paradigm (i.e., Callan et al., 2006; Hashimoto & Sakai, 2004). Indeed, while Callan et al. (2006) did not find any difference on left vOT when employing a 2-back task, Hashimoto and Sakai (2004), by asking participants to perform an audiovisual matching task, found an effect on left vOT.

[1] One can note that the coordinates of the region in left vOT varying with the strength of V-P association are more medial than coordinates of the location reported in Hashimoto and Sakai (2004), who showed that learning affected the left posterior inferior temporal gyrus (left PITG) at coordinates (-54, -51, -18) that was dissociated from an area insensitive to learning at coordinates (-36, -42, -24). The authors interpreted this dissociation as reflecting differential functional roles between these regions, with activity in left PITG reflecting the integration of newly learned visual and phonological associations, while activity in the other region reflecting the processing of already acquired associations. The discrepancy with our results could be inherent to our manipulation of V-P associations that could recruit regions involved both in new and already acquired associations.

Therefore, tasks involving greater phonological processing could induce stronger modulations of left vOT activity.

Computation of phonological information is also considered to rely on temporal regions that were significantly activated in the present study (e.g., Simos et al., 2002), with a linear effect observed in a cluster of large size (69 voxels) encompassing STG at MNI coordinates (-54, -30, 18). The STG, located in the left posterior superior temporal area (mainly Wernicke area), has been associated with an increase of activity when a task requires phonological processing, in the presence (Moore & Price, 1999) and absence of orthographic stimuli (Demonet et al., 1992; Demonet, Price, Wise, & Frackowiak, 1994). It has been shown that STG is more responsive to orthographic stimuli than objects, with an enhanced activity when the orthographic stimuli had to be read aloud (Moore & Price, 1999). Moreover, Graves, Grabowski, Mehta, and Gupta (2008) suggested that STG was implicated in accessing lexical phonology. Therefore, the linear effect observed in this cluster likely reflects a form of phonological recoding of visual stimuli.

However, we did not find any evidence for a linear effect on SMG, despite the fact that this structure has been reported as showing an increasing activity during the acquisition of new languages (Cornelissen et al., 2004; Breitenstein et al., 2005) and an increase of its white matter when learning novel speech sounds (Golestani, Paus, & Zatorre, 2007). This absence of activity related to SMG is probably due to the difference in time-scale between these studies and the present one. In the present work, the acquisition of V-P associations was achieved in a short time-window (i.e., less than a day) while language acquisition usually takes place over much longer periods of time.

Activation of Cluster 3, peaking within SMA at coordinate (-6, -9, 54) was unexpected, mainly because the present fMRI task did not require overt production of the displayed visual symbols. However, meta-analyses (Indefrey & Level, 2004; see also

Indefrey, 2011) indicate that SMA is active both in covert and overt word-reading tasks. Although its specific role in covert reading is not totally clear, Carreiras, Mechelli and Price (2006) showed that low-frequency words induced more activity in left SMA than high frequency words in a lexical decision task, and interpreted this effect as reflecting greater demands on phonological processing. Therefore, because participants in the present study had to actively maintain visual symbols in short-term memory until the presentation of the target, it is very likely that participants relied on phonological recoding and on some form of covert articulation. Results from the working memory literature also suggest that inner phonological/articulatory rehearsal increases activity of left SMA (Jonides et al., 1997). Therefore, the observed activity of left SMA in the present study likely reflects a form of inner speech (or the involvement of the phonological loop) allowing participants to actively maintain in working memory previously encountered visual symbols during a trial.

It is also interesting to note that we did not find any differential activity in the pars orpercularis of IFG, which has been reported multiple times in studies involving phonological recoding (e.g., Woodhead et al., 2014; Cai et al., 2010) and which seems to be also involved in encoding articulatory information (Klein et al., 2014). However, because participants only had to read aloud every visual symbol 7 times, this might not be sufficient enough to develop distinct articulatory representations corresponding to our four levels of phonological recoding. This could explain why we did not find a linear effect in the pars orpercularis of IFG.

Two unexpected brain regions were also active in the present experiment: the left medial frontal gyrus and the left and right posterior cingulate cortices. Previous studies have not particularly linked these regions to phonological processing or to variations in V-P associations. Their activation is therefore more likely related to the paradigm used in the fMRI experiment. Indeed, this task can be considered as a typical working memory task that requires maintaining and processing a sequence of stimuli. Variations in the strength of V-P

associations may therefore be related to variations in working memory load affecting the left medial frontal gyrus (e.g., O'Hare, Lu, Houston, Bookheimer, & Sowell, 2008). Similarly, it has been suggested that the posterior cingulate cortex and a medial frontal region incorporating portions of the medial frontal gyrus and ventral anterior cingulate cortex are components in a default mode network that is engaged during rest and disengaged during cognitive tasks (e.g., Hampson, Driesen, Skudlarski, Gore, & Constable, 2006). In the present situation, engagement of these regions could be associated with variations in processing V-P associations.

Finally, we found an effect of the strength of V-P associations mainly located in the left hemisphere in the fMRI study, while this effect appeared in the ERP study on right occipital sites between 200 and 345 ms, and on left occipital sites between 300 and 345 ms. Two lines of arguments may account for this apparent inconsistency. First, discrepancies between ERP and fMRI results are frequently reported and attributed to the specific sensitivity of each brain imaging methodology. Due to the different nature and time-scales of the recorded signals in fMRI and ERPs, the two methods do not necessarily converge (Vitacco, Brandeis, Pascual-Marqui, & Martin, 2002). While the ERP method is efficient in detecting rapid, transient and synchronous activities requiring small metabolic demands (Furey et al., 2006), fMRI is efficient in detecting sustained activities (Vitacco et al., 2002). Therefore, it has been suggested that fMRI might not be sensitive enough to detect transient activities (e.g., the N170 component, see Brem et al., 2009). Second, there are important differences in the experimental procedures used in the ERP and fMRI studies. For example, the fMRI experiment was a working memory task requiring participants to memorize series of five Katakana symbols that were presented for short durations (i.e., 200 ms per item; see Figure 2c) and that were separated by a blank screen for 2000 ms. These experimental parameters were chosen intentionally to force participants to recode phonologically the

Katakana symbols. This might explain why we observed a clearer pattern of activity mainly located in the left hemisphere in the fMRI experiment.

To conclude, the present set of results is consistent with Price and Devlin's (2011) interactive account, according to which left vOT is a brain region in which visual representations and higher-level representations (i.e., phonological representations in the present study) are integrated in the processing of visual symbols. Because STG has been previously linked to phonological recoding and is also sensitive to our present manipulation of V-P associations, it is likely that phonological recoding occurs within this region and subsequently affects activity in left vOT through top-down influences.

Acknowledgements

This study was funded by the European Research Council (ERC Advanced Grant 230313) and carried out within the Labex BLRI (ANR-11-LABX-0036). It has benefited from support from the French government, managed by the French National Agency for Research (ANR), under the project title Investments of the Future A*MIDEX (ANR-11-IDEX-0001-02).

References

Aboitiz, F., Aboitiz, S., & Garcìa, R. R. (2010). The phonological loop: A key innovation in human evolution. *Current Anthropology, 51*, S55-S65.

Ben-Shachar, M., Dougherty, R. F., & Wandell, B. A. (2007). White matter pathways in reading. *Current Opinion in Neurobiology*, *17*(2), 258–270.

Ben-Shachar, M., Dougherty, R. F., Deutsch, G. K., & Wandell, B. A. (2011). The development of cortical sensitivity to visual word forms. *Journal of Cognitive Neuroscience*, *23*(9), 2387-2399.

Bolger, D. J., Perfetti, C. A., & Schneider, W. (2005). Cross-cultural effect on the brain revisited: Universal structures plus writing system variation. *Human Brain Mapping*, *25*(1), 92-104.

Breitenstein, C., Jansen, A., Deppe, M., Foerster, A.-F., Sommer, J., Wolbers, T., & Knecht, S. (2005). Hippocampus activity differentiates good from poor learners of a novel lexicon. *Neuroimage*, *25*(3), 958–968.

Brem, S. Bach, S. Kujala, J. V., Maurer, U., Lyytinen, H., Richardson, U., Brandeis, D. (2013). An Electrophysiological Study of Print Processing in Kindergarten: The Contribution of the Visual N1 as a Predictor of Reading Outcome. *Developmental Neuropsychology*, 38(8), 567-594.

Cai, Q., Paulignan, Y., Brysbaert, M., Ibarrola, D., & Nazir, T. A. (2010). The left ventral occipito-temporal response to words depends on language lateralization but not on visual familiarity. *Cerebral Cortex*, *20*(5), 1153–1163.

Callan, A. M., Callan, D. E., & Masaki, S. (2005). When meaningless symbols become letters: neural activity change in learning new phonograms. *Neuroimage*, *28*(3), 553–562.

Carreiras, M., Armstrong, B. C., Perea, M., & Frost, R. (2014). The what, when, where, and

how of visual word recognition. *Trends in Cognitive Sciences*, *18*(2), 90–98.

Carreiras, M., Perea, M., Gil-López, C., Mallouh, R. A., & Salillas, E. (2013). Neural Correlates of Visual versus Abstract Letter Processing in Roman and Arabic Scripts. *Journal of Cognitive Neuroscience*, *25*(11), 1975-1985.

Carreiras, M., Mechelli, A., & Price, C. J. (2006). Effect of word and syllable frequency on activation during lexical decision and reading aloud. *Human Brain Mapping*, *27*(12), 963-972.

Church, J. A., Balota, D. A., Petersen, S. E., & Schlaggar, B. L. (2011). Manipulation of Length and Lexicality Localizes the Functional Neuroanatomy of Phonological Processing in Adult Readers. *Journal of Cognitive Neuroscience*, *23*(6), 1475–1493.

Cohen, L., Dehaene, S., Naccache, L., Lehéricy, S., Dehaene-Lambertz, G., Hénaff, M. A., & Michel, F. (2000). The visual word form area Spatial and temporal characterization of an initial stage of reading in normal subjects and posterior split-brain patients. *Brain*, *123*(2), 291-307.

Cohen, L., Lehericy, S., Chochon, F., Lemer, C., Rivaud, S., & Dehaene, S. (2002). Language- specific tuning of visual cortex? Functional properties of the visual word form area. *Brain, 125*, 1054–1069.

Cohen, M. X. (2014). *Analyzing neural time series data: theory and practice*. MIT Press.

Cornelissen, K., Laine, M., Renvall, K., Saarinen, T., Martin, N., & Salmelin, R. (2004). Learning new names for new objects: Cortical effects as measured by magnetoencephalography. *Brain and Language*, *89*(3), 617–622.

Dehaene, S., & Cohen, L. (2011). The unique role of the visual word form area in reading. *Trends in Cognitive Sciences*, *15*(6), 254-262.

Dehaene, S., Cohen, L., Sigman, M., & Vinckier, F. (2005). The neural code for written words: a proposal. *Trends in Cognitive Sciences*, *9*(7), 335-341.

Dehaene, S., Le Clec'H, G., Poline, J. B., Le Bihan, D., & Cohen, L. (2002). The visual word form area: a prelexical representation of visual words in the fusiform gyrus. *Neuroreport*, *13*(3), 321-325.

Dehaene, S., Naccache, L., Cohen, L., Le Bihan, D., Mangin, J. F., Poline, J. B., & Rivière, D. (2001). Cerebral mechanisms of word masking and unconscious repetition priming. *Nature Neuroscience*, *4*(7), 752-758.

Delorme, A., & Makeig, S. (2004). EEGLAB: an open source toolbox for analysis of single-trial EEG dynamics including independent component analysis. *Journal of Neuroscience Methods*, *134*(1), 9-21.

Delorme, A., Sejnowski, T., & Makeig, S. (2007). Enhanced detection of artifacts in EEG data using higher-order statistics and independent component analysis. *Neuroimage*, *34*(4), 1443-1449.

Demonet, J. F., Chollet, F., Ramsay, S., Cardebat, D., Nespoulous, J. L., Wise, R., Rascol, A., & Frackowiak, R. (1992). The anatomy of phonological and semantic processing in normal subjects. *Brain*, *115*(6), 1753-1768.

Demonet, J. F., Price, C., Wise, R., & Frackowiak, R. S. J. (1994). Differential activation of right and left posterior sylvian regions by semantic and phonological tasks: a positron-emission tomography study in normal human subjects. *Neuroscience Letters*, *182*(1), 25-28.

Flowers, D. L., Jones, K., Noble, K., VanMeter, J., Zeffiro, T. A., Wood, F. B., & Eden, G. F. (2004). Attention to single letters activates left extrastriate cortex. *Neuroimage*, *21*(3), 829–839.

Foulin, J.-N. (2005). Why is letter-name knowledge such a good predictor of learning to read? *Reading and Writing,18(2)*, 129-155.

Garrett, A. S., Flowers, D. L., Absher, J. R., Fahey, F. H., Gage, H. D., Keyes, J. W., Porrino,

L. J., et al. (2000). Cortical activity related to accuracy of letter recognition. *Neuroimage*, *11*(2), 111–123.

Gitelman, D. R., Nobre, A. C., Sonty, S., Parrish, T. B., & Mesulam, M.-M. (2005). Language network specializations: An analysis with parallel task designs and functional magnetic resonance imaging. *Neuroimage*, *26*(4), 975–985.

Golestani, N., Paus, T., & Zatorre, R. J. (2002). Anatomical correlates of learning novel speech sounds. *Neuron*, *35*(5), 997-1010.

Grainger, J. Kiyonaga, K., & Holcomb, P.J. (2006). The time-course of orthographic and phonological code activation. *Psychological Science*, *17*, 1021-1026.

Grainger, J., Rey, A., & Dufau, S. (2008). Letter perception: from pixels to pandemonium. *Trends in Cognitive Sciences*, *12*(10), 381–387.

Graves, W. W., Grabowski, T. J., Mehta, S., & Gupta, P. (2008). The left posterior superior temporal gyrus participates specifically in accessing lexical phonology. *Journal of Cognitive Neuroscience*, *20*(9), 1698–1710.

Grill-Spector, K., & Malach, R. (2004). The human visual cortex. *Annual Review of Neuroscience*, *27*, 649–677.

Hagoort, P., Indefrey, P., Brown, C., Herzog, H., Steinmetz, H., & Seitz, R. (1999). The neural circuitry involved in the reading of German words and pseudowords: a PET study. *Journal of Cognitive Neuroscience, 11*(4), 383-398.

Hampson, M., Driesen, N. R., Skudlarski, P., Gore, J. C., & Constable, R. T. (2006). Brain connectivity related to working memory performance. *The Journal of Neuroscience*, *26*(51), 13338-13343.

Hashimoto, R., & Sakai, K. (2004). Learning letters in adulthood: Direct visualization of cortical plasticity for forming a new link between orthography and phonology. *Neuron*, *42*(2), 311–322.

Indefrey, P. (2011) The spatial and temporal signatures of word production components: A critical update. *Frontiers in Psychology,* 2:255. doi:10.3389/fpsyg.2011.00255.

Indefrey, P., & Levelt, W. J. (2004). The spatial and temporal signatures of word production components. *Cognition*, *92*(1), 101-144.

James, K. H., & Gauthier, I. (2006). Letter processing automatically recruits a sensory–motor brain network. *Neuropsychologia*, *44*(14), 2937–2949.

Jobard, G., Crivello, F., & Tzourio-Mazoyer, N. (2003). Evaluation of the dual route theory of reading: a metanalysis of 35 neuroimaging studies. *Neuroimage*, *20*(2), 693–712.

Jonides, J., Schumacher, E., Smith, E., Lauber, E., Awh, E., Minoshima, S., & Koeppe, R. (1997). Verbal working memory load affects regional brain activation as measured by PET. *Journal of Cognitive Neuroscience, 9*(4), 462-475.

Joseph, J. E., Cerullo, M. A., Farley, A. B., Steinmetz, N. A., & Mier, C. R. (2006). fMRI correlates of cortical specialization and generalization for letter processing. *Neuroimage*, *32*(2), 806-820.

Joseph, J. E., Gathers, A. D., & Piper, G. A. (2003). Shared and dissociated cortical regions for object and letter processing. *Cognitive Brain Research*, *17*(1), 56-67.

Kherif, F., Josse, G., & Price, C. J. (2011). Automatic top-down processing explains common left occipito-temporal responses to visual words and objects. *Cerebral Cortex, 21*(1), 103–114.

Klein, M., Grainger, J., Wheat, K. L., Millman, R. E., Simpson, M. I. G., Hansen, P. C., & Cornelissen, P. L. (2015). Early activity in Broca's Area during reading reflects fast access to articulatory codes from print. *Cerebral Cortex*. doi.org/10.1093/cercor/bht350

Levy, J., Pernet, C., Treserras, S., Boulanouar, K., Berry, I., Aubry, F., Demoulins, T., & Celsis, P. (2008). Piecemeal recruitment of left-lateralized brain areas during reading: A spatio-functional account. *Neuroimage*, *43*(3), 581–591.

Liu, C., Zhang, W. T., Tang, Y. Y., Mai, X. Q., Chen, H. C., Tardif, T., & Luo, Y. J. (2008). The visual word form area: evidence from an fMRI study of implicit processing of Chinese characters. *Neuroimage*, *40*(3), 1350-1361.

Li, X., Zhou, P., & Aruin, A. S. (2007). Teager–Kaiser energy operation of surface EMG improves muscle activity onset detection. *Annals of Biomedical Engineering*, *35*(9), 1532-1538.

Logothetis, N. K., & Sheinberg, D. L. (1996). Visual object recognition. *Annual review of neuroscience*, *19*(1), 577-621.

Madec, S., Rey, A., Dufau, S., Klein, M., & Grainger, J. (2012). The time course of visual letter perception. *Journal of Cognitive Neuroscience*, *24*(7), 1645-1655.

Mainy, N., Jung, J., Baciu, M., Kahane, P., Schoendorff, B., Minotti, L., Hoffmann, D., Bertrand, O., & Lachaux, J.P. (2008). Cortical dynamics of word recognition. *Human Brain Mapping*, *29*(11), 1215–1230.

Makeig, S., Bell, A. J., Jung, T. P., & Sejnowski, T. J. (1996). Independent component analysis of electroencephalographic data. *Advances in Neural Information Processing Systems*, 145-151.

Mano, Q. R., Humphries, C., Desai, R. H., Seidenberg, M. S., Osmon, D. C., Stengel, B. C., & Binder, J. R. (2013). The role of left occipitotemporal cortex in reading: reconciling stimulus, task, and lexicality effects. *Cerebral Cortex, 23*(4), 988–1001.

Maris, E., & Oostenveld, R. (2007). Nonparametric statistical testing of EEG-and MEG-data. *Journal of Neuroscience Methods*, *164*(1), 177-190.

Maurer, U., Blau, V. C., Yoncheva, Y. N., & McCandliss, B. D. (2010). Development of visual expertise for reading: rapid emergence of visual familiarity for an artificial script. *Developmental Neuropsychology*, *35*(4), 404-422.

Maurer U, Brem S, Bucher K, Brandeis D. Emerging neurophysiological specialization for

letter strings. Journal of Cognitive Neuroscience. 2005; 17(10):1532–1552.

McCandliss, B. D., Cohen, L., & Dehaene, S. (2003). The visual word form area: expertise for reading in the fusiform gyrus. *Trends in Cognitive Sciences*, *7*(7), 293-299.

Mei, L., Xue, G., Lu, Z. L., He, Q., Zhang, M., Xue, F., Chen, C., & Dong, Q. (2013). Orthographic transparency modulates the functional asymmetry in the fusiform cortex: an artificial language training study. *Brain and Language*, *125*(2), 165-172.

Moore, C. J., & Price, C. J. (1999). Three distinct ventral occipitotemporal regions for reading and object naming. *Neuroimage*, *10*(2), 181-192.

Nichols, T. E., & Holmes, A. P. (2002). Nonparametric permutation tests for functional neuroimaging: a primer with examples. *Human Brain Mapping*, *15*(1), 1-25.

Nunez, P. L., & Srinivasan, R. (2006). *Electric fields of the brain: the neurophysics of EEG*. Oxford university press.

O'Hare, E. D., Lu, L. H., Houston, S. M., Bookheimer, S. Y., & Sowell, E. R. (2008). Neurodevelopmental changes in verbal working memory load-dependency: An fMRI investigation. *Neuroimage*, *42*(4), 1678–1685.

Olulade, O. A., Flowers, D. L., Napoliello, E. M., & Eden, G. F. (2013). Developmental differences for word processing in the ventral stream. *Brain and Language*, *125*(2), 134–145.

Orr, J. M., & Banich, M. T. (2014). The neural mechanisms underlying internally and externally guided task selection. *Neuroimage*, *84*, 191-205.

Paulesu, E., McCrory, E., Fazio, F., Menoncello, L., Brunswick, N., Cappa, S. F., Cotelli M., Cossu G., Corte F., Lorusso M., Pesenti S., Gallagher A., Perani D., Price C., Frith C.D., Frith U. (2000). A cultural effect on brain function. *Nature Neuroscience*, *3*(1), 91-96.

Pedregosa, F., Varoquaux, G., Gramfort, A., Michel, V., Thirion, B., Grisel, O., Blondel, M.,

Prettenhofer, P., Weiss, R., Dubourg, V., Vanderplas, J., Passos, A., Cournapeau, D., Brucher, M., Perrot, M., & Duchesnay, E. (2011). Scikit-learn: Machine learning in Python. *Journal of Machine Learning Research, 12*, 2825–2830.

Pegado, F., Nakamura, K., Cohen, L., & Dehaene, S. (2011). Breaking the symmetry: mirror discrimination for single letters but not for pictures in the Visual Word Form Area. *Neuroimage*, *55*(2), 742-749.

Perrin, F., Pernier, J., Bertrand, O., & Echallier, J. F. (1989). Spherical splines for scalp potential and current density mapping. *Electroencephalography and clinical Neurophysiology*, *72*(2), 184-187.

Pernet, C., Celsis, P., & Demonet, J.-F. (2005). Selective response to letter categorization within the left fusiform gyrus. *Neuroimage*, *28*(3), 738–744.

Pernet, C. R., Chauveau, N., Gaspar, C., & Rousselet, G. A. (2011). LIMO EEG: a toolbox for hierarchical LInear MOdeling of ElectroEncephaloGraphic data. *Computational Intelligence and Neuroscience*, *2011*, 3.

Petit, J. P., Midgley, K. J., Holcomb, P. J., & Grainger, J. (2006). On the time course of letter perception: A masked priming ERP investigation. *Psychonomic Bulletin & Review*, *13*(4), 674-681.

Polk, T. A., & Farah, M. J. (1998). The neural development and organization of letter recognition: Evidence from functional neuroimaging, computational modeling, and behavioral studies. *Proceedings of the National Academy of Sciences*, *95*(3), 847-852.

Polk, T. A., & Farah, M. J. (2002). Functional MRI evidence for an abstract, not perceptual, word-form area. *Journal of Experimental Psychology: General*, *131*(1), 65-72.

Price, C. J. (2000). The anatomy of language: contributions from functional neuroimaging. *Journal of Anatomy*, *197*(3), 335-359.

Price, C. J. (2013). Current themes in neuroimaging studies of reading. *Brain and Language*,

125(2), 131–133.

Price, C. J., & Devlin, J. T. (2003). The myth of the visual word form area. *Neuroimage*, *19*(3), 473–481.

Price, C. J., & Devlin, J. T. (2011). The Interactive Account of ventral occipitotemporal contributions to reading. *Trends in Cognitive Sciences*, *15*(6), 246–253.

Price, C. J., & Mechelli, A. (2005). Reading and reading disturbance. *Current Opinion in Neurobiology*, *15*(2), 231-238.

Price, C. J., Moore, C. J., Humphreys, G. W., & Wise, R. J. S. (1997). Segregating semantic from phonological processes during reading. *Journal of Cognitive Neuroscience*, *9*(6), 727-733.

Price, C. J., Wise, R. J., & Frackowiak, R. S. (1996): Demonstrating the implicit processing of visually presented words and pseudowords. *Cerebral Cortex, 6*, 62–70.

Pugh, K. R., Shaywitz, B. A., Shaywitz, S. E., Constable, R. T., Skudlarski, P., Fulbright, R. K., Bronen, R. A., Shankweiler, D. P., Katz, L., Fletcher, J. M., & Gore, J. C. (1996). Cerebral organization of component processes in reading. *Brain*, *119*(4), 1221-1238.

Rey, A., Dufau, S., Massol, S., & Grainger, J. (2009). Testing computational models of letter perception with item-level event-related potentials. *Cognitive Neuropsychology*, *26*(1), 7-22.

Rolls, E. T. (2000). Functions of the primate temporal lobe cortical visual areas in invariant visual object and face recognition. *Neuron*, *27*(2), 205-218.

Rumsey, J. M., Horwitz, B., Donohue, B. C., Nace, K., Maisog, J. M., & Andreason, P. (1997). Phonological and orthographic components of word recognition. A PET-rCBF study. *Brain*, *120*(5), 739-759.

Rothlein, D., & B. Rapp (2014). The similarity structure of distributed neural responses reveals the multiple representations of letters. *Neuroimage,89*, 331-344.

Sandak, R., Mencl, W. E., Frost, S. J., Rueckl, J. G., Katz, L., Moore, D. L., Mason, S. A., Fulbright, R. K., Constable, T., & Pugh, K. R. (2004). The neurobiology of adaptive learning in reading: A contrast of different training conditions. *Cognitive, Affective, & Behavioral Neuroscience*, *4*(1), 67-88.

Schlaggar, B. L., & McCandliss, B. D. (2007). Development of neural systems for reading. *Annual Review of Neuroscience*, *30*(1), 475–503.

Seghier, M. L., & Price, C. J. (2011). Explaining left lateralization for words in the ventral occipitotemporal cortex. *The Journal of Neuroscience*, *31*(41), 14745-14753.

Sevostianov, A., Horwitz, B., Nechaev, V., Williams, R., Fromm, S., & Braun, A. R. (2002). fMRI study comparing names versus pictures of objects. *Human brain mapping*, *16*(3), 168-175.

Simos, P. G., Breier, J. I., Fletcher, J. M., Foorman, B. R., Castillo, E. M., & Papanicolaou, A. C. (2002). Brain mechanisms for reading words and pseudowords: an integrated approach. *Cerebral Cortex*, *12*(3), 297-305.

Simos, P. G., Rezaie, R., Fletcher, J. M., & Papanicolaou, A. C. (2013). Time- constrained functional connectivity analysis of cortical networks underlying phonological decoding in typically developing school-aged children: A magnetoencephalography study. *Brain & Language, 125(2)*, 156–164.

Smith, S. M., & Nichols, T. E. (2009). Threshold-free cluster enhancement: addressing problems of smoothing, threshold dependence and localisation in cluster inference. *Neuroimage*, *44*(1), 83-98.

Song, Y., Tian, M., & Liu, J. (2012). Top-down processing of symbolic meanings modulates the visual word form area. *The Journal of Neuroscience*, *32*(35), 12277-12283.

Stoeckel, C., Gough, P. M., Watkins, K. E., & Devlin, J. T. (2009). Supramarginal gyrus involvement in visual word recognition. *Cortex*, *45*(9), 1091–1096.

Tarkiainen, A., Cornelissen, P. L., & Salmelin, R. (2002). Dynamics of visual feature analysis and object-level processing in face versus letter-string perception. *Brain*, *125*(5), 1125-1136.

Tarkiainen, A., Helenius, P., Hansen, P. C., Cornelissen, P. L., & Salmelin, R. (1999). Dynamics of letter string perception in the human occipitotemporal cortex. *Brain*, *122*(11), 2119-2132.

Treiman, R., & Kessler, B. (2004). The role of letter names in the acquisition of literacy. *Advances in child development and behavior*, *31*, 105-135.

Turkeltaub, P. E., Eden, G. F., Jones, K. M., & Zeffiro, T. A. (2002). Meta-Analysis of the Functional neuroanatomy of single-word reading: method and validation. *Neuroimage*, *16*(3), 765–780.

Twomey, T., Duncan, K. J. K., Price, C. J., & Devlin, J. T. (2011). Top-down modulation of ventral occipito-temporal responses during visual word recognition. *Neuroimage*, *55*(3), 1242–1251.

Vandermosten, M., Boets, B., Wouters, J., & Ghesquière, P. (2012). A qualitative and quantitative review of diffusion tensor imaging studies in reading and dyslexia. *Neuroscience and Biobehavioral Reviews*, *36*(6), 1532–1552.

Van Essen, D. C., Glasser, M. F., Dierker, D. L., Harwell, J., & Coalson, T. (2012). Parcellations and hemispheric asymmetries of human cerebral cortex analyzed on surface-based atlases. *Cerebral Cortex*, *22*(10), 2241-2262.

Vigneau, M., Beaucousin, V., Hervé, P. Y., Duffau, H., Crivello, F., Houdé, O., Mazoyer, B., Tzourio-Marzoyer, N. (2006). Meta-analyzing left hemisphere language areas: phonology, semantics, and sentence processing. *Neuroimage*, *30*(4), 1414–1432.

Vogel, A. C., Petersen, S. E., & Schlaggar, B. L. (2012). The left occipitotemporal cortex does not show preferential activity for words. *Cerebral Cortex*, *22*(12), 2715–2732.

Wilcox, R. (2011). *Modern statistics for the social and behavioral sciences: A practical introduction*. CRC press.

Wilson, L. B., Tregellas, J. R., Slason, E., Pasko, B. E., & Rojas, D. C. (2011). Implicit phonological priming during visual word recognition. *Neuroimage*, *55*(2), 724–731.

Wong, A. C., Gauthier, I., Woroch, B., Debuse, C., & Curran, T. (2005). An early electrophysiological response associated with expertise in letter perception. *Cognitive, Affective, & Behavioral Neuroscience*, *5*(3), 306-318.

Wong, A. C. N., Jobard, G., James, K. H., James, T. W., & Gauthier, I. (2009). Expertise with characters in alphabetic and nonalphabetic writing systems engage overlapping occipito-temporal areas. *Cognitive Neuropsychology*, *26*(1), 111–127.

Woodhead, Z. V. J., Barnes, G. R., Penny, W., Moran, R., Teki, S., Price, C. J., & Leff, A. P. (2014). Reading front to back: MEG evidence for early feedback effects during word recognition. *Cerebral Cortex*, *24*(3), 817–825.

Woodhead, Z. V., Brownsett, S. L., Dhanjal, N. S., Beckmann, C., & Wise, R. J. (2011). The visual word form system in context. *The Journal of Neuroscience*, *31*(1), 193-199.

Woodhead, Z. V. J., Penny, W., Barnes, G. R., Crewes, H., Wise, R. J. S., Price, C. J., & Leff, A. P. (2013). Reading therapy strengthens top-down connectivity in patients with pure alexia. *Brain*, *136*(8), 2579–2591.

Wright, N. D., Mechelli, A., Noppeney, U., Veltman, D. J., Rombouts, S. A. R. B., Glensman, J., Haynes, J. D., & Price, C. J. (2008). Selective activation around the left occipito-temporal sulcus for words relative to pictures: Individual variability or false positives? *Human Brain Mapping*, *29*(8), 986–1000.

Xue, G., Chen, C., Jin, Z., & Dong, Q. (2006). Language experience shapes fusiform activation when processing a logographic artificial language: An fMRI training study. *Neuroimage*, *31*(3), 1315–1326.

Yeatman, J. D., Rauschecker, A. M., & Wandell, B. A. (2013). Anatomy of the visual word form area: Adjacent cortical circuits and long-range white matter connections. *Brain and Language*, *125*(2), 146–155.

Yeatman, J. D., Weiner, K. S., Pestilli, F., Rokem, A., Mezer, A., & Wandell, B. A. (2014). The vertical occipital fasciculus: A century of controversy resolved by in vivo measurements. *Proceedings of the National Academy of Sciences, 111*, 5214–5223.

Yoncheva, Y. N., Blau, V. C., Maurer, U., & McCandliss, B. D. (2010). Attentional focus during learning impacts N170 ERP responses to an artificial script. *Developmental Neuropsychology*, *35*(4), 423-445.

Yum, Y.N., Holcomb, P.J., & Grainger, J. (2011). Words and pictures: An electrophysiological investigation of domain specific processing in native Chinese and English speakers. *Neuropsychologia*, 49, 1910-1922.

Appendix A:
Testing the parametric modulation of performance using a linear contrast

At the individual level, we first calculated median reaction times (RTs) and mean accuracies (ACCs) of responses, for each of the three parts of the learning phase and for each of the four learning conditions. Note that no trials were rejected.

We then integrated these central tendency measures in linear contrasts as defined by:

$$L_{sRT} = -2Md_{sL1} - Md_{sL2} + Md_{sL3} + 2Md_{sL4}$$

and

$$L_{sACC} = -2\bar{x}_{sL1} - \bar{x}_{sL2} + \bar{x}_{sL3} + 2\bar{x}_{sL4}$$

with Md_{sL1}, Md_{sL2}, Md_{sL3}, Md_{sL4} corresponding respectively to the median RT of L1, L2, L3, L4 for participant *s*, and $\bar{x}_{sL1}$, $\bar{x}_{sL2}$, $\bar{x}_{sL3}$, $\bar{x}_{sL4}$ corresponding respectively to mean accuracies of L1, L2, L3, L4 for participant *s*. Weights associated to each condition [-2 -1 1 2] were defined according to distances between the strength of the V-P associations for L1, L2, L3, and L4 obtained by the experimental manipulation.

At the group level, we assessed the significance of linear contrasts by using a one sample t-test, with the null hypotheses defined by$\acute{L}_{RT} = 0$ and $\acute{L}_{Acc} = 0$. We employed a bootstrap-t approach (Wilcox, 2011), in which subjects are drawn randomly with replacement. Dependent variables (RTs or ACCs) were first centered around the means, and for each bootstrap (B=1000) a one sample t-test was performed. Results from this t-test under the null hypothesis were stored for each bootstrap. As a result, a distribution of T values under H0 was estimated, therefore allowing the estimation of the 0.025 and 0.975 quantiles (corresponding to a bilateral test with $p < .05$). We then tested if the observed t-values on the original data belonged to the extremes of these quantiles.

Appendix B:
Number of trials included in each condition for the ERP analysis

	Part 1				Part 2				Part 3			
	L1	L2	L3	L4	L1	L2	L3	L4	L1	L2	L3	L4
1	68	68	66	64	69	70	64	63	60	66	69	61
2	52	56	50	56	52	52	57	54	52	45	50	47
3	52	54	60	55	52	52	52	51	47	52	54	58
4	66	69	70	69	68	66	66	69	62	62	59	65
5	57	62	63	62	55	53	53	56	64	58	62	62
6	57	52	50	55	54	60	56	53	59	58	57	58
7	65	65	67	67	55	46	50	41	52	49	50	48
8	60	62	60	61	58	64	59	63	66	62	61	66
9	56	51	52	51	51	48	58	45	61	54	59	55
10	51	54	57	52	52	48	47	45	61	63	59	65
11	57	56	56	54	62	62	65	69	37	52	36	45
12	46	37	40	44	53	45	47	41	49	53	46	47
13	64	64	65	62	62	63	62	56	55	44	48	58
14	55	56	61	49	56	57	52	56	57	60	54	61
15	-	-	-	-	-	-	-	-	-	-	-	-
16	56	54	55	58	51	54	53	58	56	66	58	63
17	43	36	41	41	39	39	41	50	39	43	48	44
18	-	-	-	-	-	-	-	-	-	-	-	-
19	37	44	38	43	40	41	37	41	35	30	41	36
20	51	53	53	52	59	65	61	55	59	62	60	60
21	63	67	62	61	70	58	61	66	50	56	54	57
22	43	48	42	54	56	59	59	57	53	55	51	50
23	-	-	-	-	-	-	-	-	-	-	-	-
24	61	54	58	67	62	59	62	50	56	63	55	59
M	55.6	55.4	55.3	55	56	56	55	55	54	55	54	55

Table 1: Results of the 2AFC task. DV = Dependent Variable; T = observed t-values calculated on the original sample; p = probability that a t-value obtained by bootstrap under H0 is above or below the observed t-value; L = mean of the observed linear contrasts; CI = Confidence Intervals.

Day	Part	DV	T	p	$\acute{L}$	CI (95%)
1	1	RT	-5.68	< .001	-360	[-495; -226]
		ACC	6.51	< .001	0.46	[0.31; 0.61]
	2	RT	-9.57	< .001	-754	[-924; -584]
		ACC	11.38	< .001	0.53	[0.43; 0.62]
	3	RT	-7.02	< .001	-510	[-672; -347]
		ACC	5.62	< .001	0.26	[0.16; 0.36]
2	-	RT	-8.44	< .001	-453	[-564; -341]
		ACC	4.68	0.002	0.18	[0.09; 0.26]

Table 2: Results of the naming task.

Day	Part	DV	T	p	$\acute{L}$	CI (95%)
1	1	RT	-4.32	0.002	-2061	[-3182; -939]
		ACC	10.39	< .001	0.9	[0.72; 1.08]
	2	RT	-6.03	< .001	-1459	[-1991; -928]
		ACC	11.21	< .001	1.06	[0.86; 1.26]
	3	RT	-3.85	0.003	-931	[-1456; -406]
		ACC	5.42	< .001	0.59	[0.36; 0.81]
2	-	RT	-3.08	0.004	-463	[-772; -154]
		ACC	4.24	0.002	0.5	[0.24; 0.76]

Table 3: Significant clusters for the linear contrast [-2 -1 1 2] associated to L1, L2, L3 and L4 conditions. Reported values are for the peak of activation, local maxima and for each cluster. Due to the size of cluster 3 (59 voxels), local maxima within this cluster are indicated. Coordinates are in MNI space.

Cluster #	Anatomical label	Number of voxels	t-values at peak coordinates	t-values at global maxima	Coordinates (MNI)		
					x	y	z
1	Left fusiform gyrus	31	5.21	-	-33	-42	-18
2	Left superior temporal gyrus	69	5.01	5.01	-54	-30	18
				4.37	-36	-36	21
				3.96	-48	-42	12
3	Left supplementary motor area	33	6.01	-	-6	-9	54
4	Left frontal superior medial	55	4.71	4.71	-6	63	18
				4.64	0	57	15
				4.29	-9	57	12
5	Posterior cingulate	54	4.40	4.40	6	-63	15
				4.02	-15	-57	9
				3.91	-6	-54	15

Figure captions

Figure 1: a) Overview of the experiment over Day 1 and Day 2. b) Katakana symbols used in the experiment, with their associated sound composed of a consonant (in row) and a vowel (in column). Shades of gray differentiate the four groups of Katakana symbols.

Figure 2: a) Trial description for the 2AFC task. ERP recording involved 12 learning sessions of 92 trials (for a duration of approximately 5 to 6 minutes), in which participants learned the names of visual symbols through this 2AFC task. Over the 12 learning sessions, every visual symbol from L1, L2, L3 and L4 was presented in 36 trials. b) Trial description for the naming task. Naming task occurred after learning sessions 2, 4, 6, 8, 10 and 12. Every visual symbol was presented once during this task. c) Block description for the matching task during the fMRI experiment. The fMRI procedure involved 4 functional runs. Each functional run embedded 6 blocks, half of them corresponding to a target present block. Duration of each functional run was approximately 8 minutes.

Figure 3: Descriptive behavioral results for the 2AFC and naming tasks. L1, L2, L3 and L4 correspond to the various learning conditions as defined by the strengths of V-P associations (see Method for additional information). C corresponds to the letter condition. Part (1, 2, and 3) and Day (1 and 2) of the experiment are indicated in column. Mean RTs and mean ACCs for the 2AFC are provided in Row 1 and 2, and mean RTs and mean ACCs for the naming task are provided in Row 3 and 4. All CI are given at the alpha level 95%.

Figure 4: ERPs results. a) Uncorrected and corrected results testing for a linear effect of the learning conditions on ERPs, on the entire spatial and temporal dimensions. Time 0 corresponds to the visual presentation of Katakana symbols. b) Illustration of the linear effect on electrode P8. c) Mean linear effect at the group level and its associated CI at 95% for electrode P8.

Figure 5: fMRIs results for a linear effect of the learning conditions, with maximum intensity projection of significant t-values. Circled numbers correspond to clusters showing significant linear effects.

Figure 6: fMRIs results. Slice view of the peak activations for the three main significant clusters (from Figure 5 and Table 3), displayed on the T1 underlay from the Conte69 Atlas (Van Essen, Glasser, Dierker, Harwell, & Coalson, 2012; implemented on the Connectome workbench software version 1.0). Cluster 1 corresponds to left fusiform gyrus, Cluster 2 corresponds to left superior temporal gyrus, and Cluster 3 corresponds to left supplementary motor area. For descriptive purposes, we also represented the mean MR signals extracted from whole clusters by condition. Additionally, mean linear contrasts values computed over clusters are given. All CI are given at the alpha level 95%.

a)

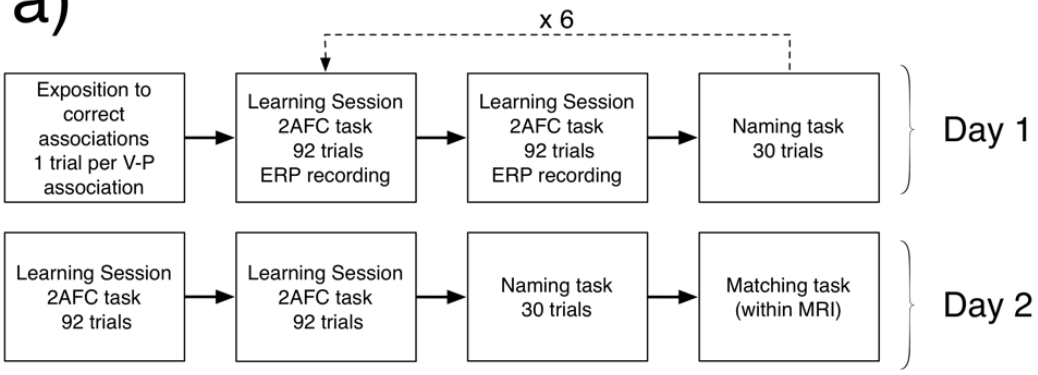

b)

	/a/	/i/	/e/	/o/
/k/	ウ	ソ	ネ	ス
/l/	リ	オ	ヲ	サ
/t/	い	カ	マ	ラ
/b/	フ	モ	ヌ	レ
/m/	タ	つ	ハ	メ
/ʁ/	ル	ム	ア	ト

Figure 1

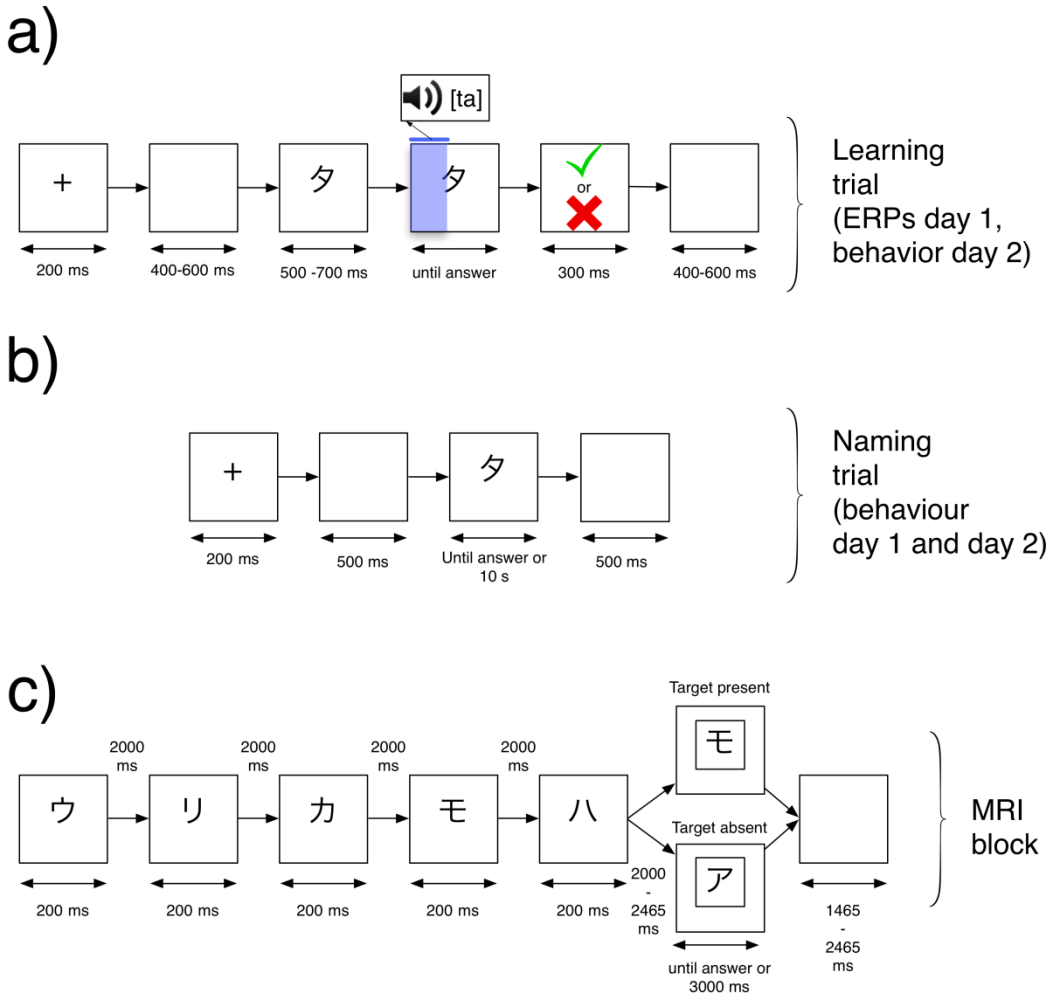
a)
[ta]
+
タ
タ
or
200 ms
400-600 ms
500 -700 ms
until answer
300 ms
400-600 ms
Learning trial (ERPs day 1, behavior day 2)
b)
+
タ
200 ms
500 ms
Until answer or 10 s
500 ms
Naming trial (behaviour day 1 and day 2)
c)
2000 ms
ウ
リ
カ
モ
ハ
200 ms
Target present
モ
Target absent
ア
2000 - 2465 ms
until answer or 3000 ms
1465 - 2465 ms
MRI block

Figure 2

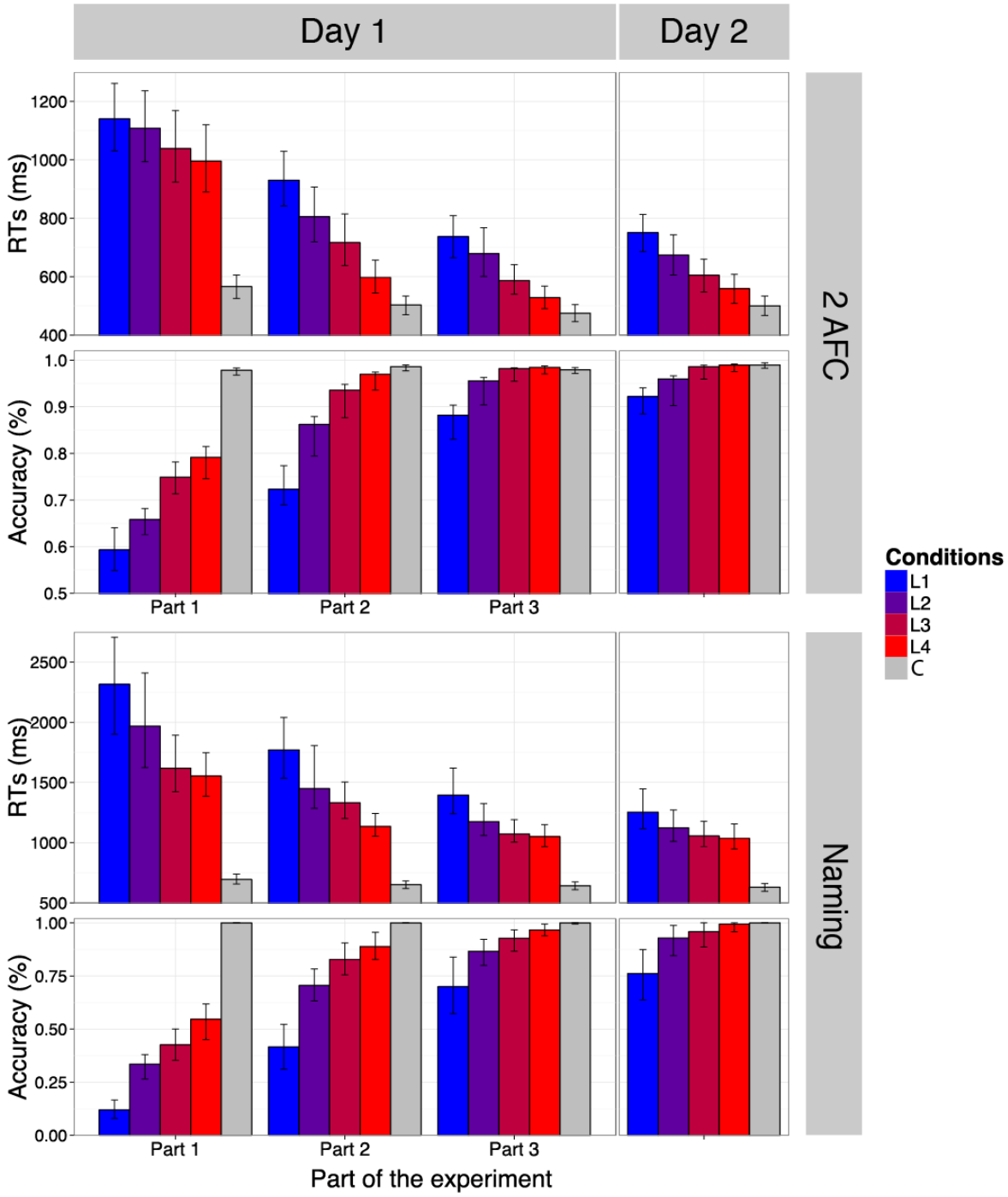
Day 1
Day 2
2 AFC
Naming
RTs (ms)
Accuracy (%)
Part 1
Part 2
Part 3
Part of the experiment
Conditions
L1
L2
L3
L4
C

Figure 3

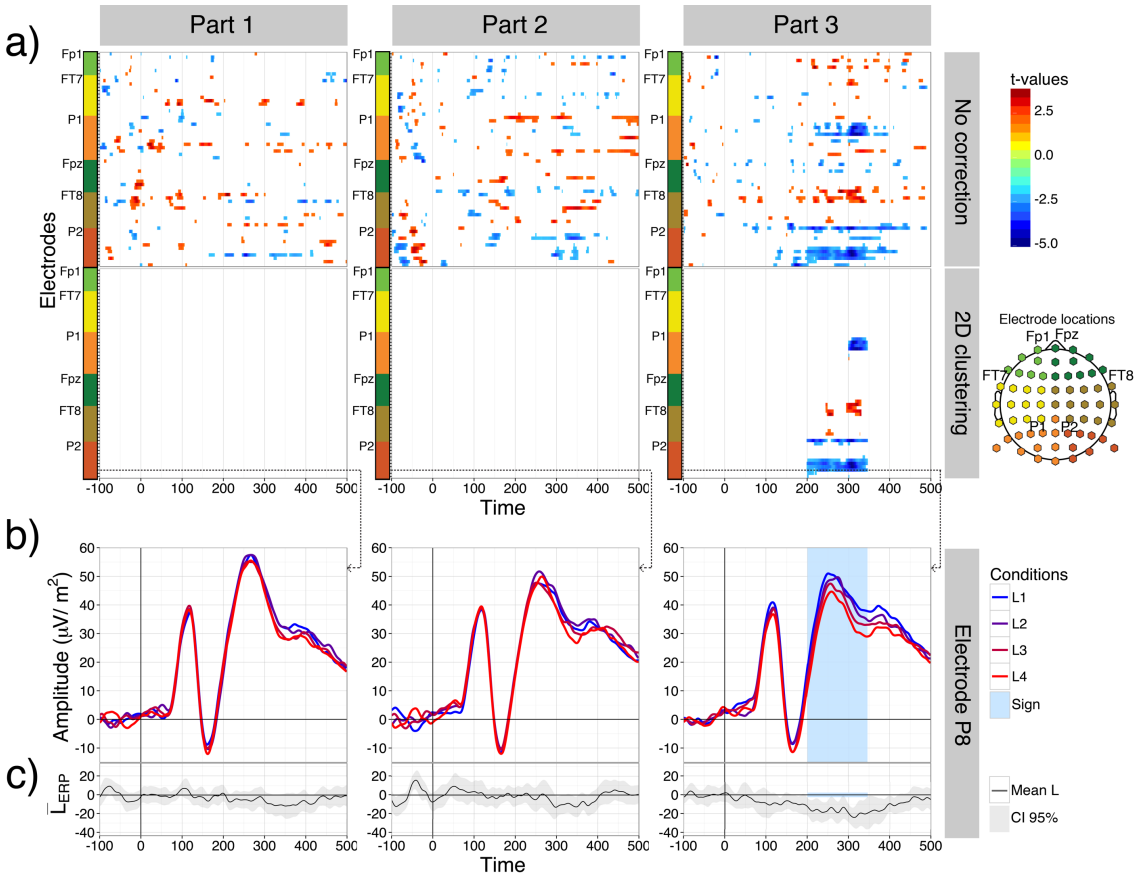
a)
Part 1
Part 2
Part 3
No correction
2D clustering
Electrodes
Fp1
FT7
P1
Fpz
FT8
P2
t-values
2.5
0.0
-2.5
-5.0
Electrode locations
Time
b)
Amplitude (μV/ m²)
Electrode P8
Conditions
L1
L2
L3
L4
Sign
c)
LERP
Mean L
CI 95%

Figure 4

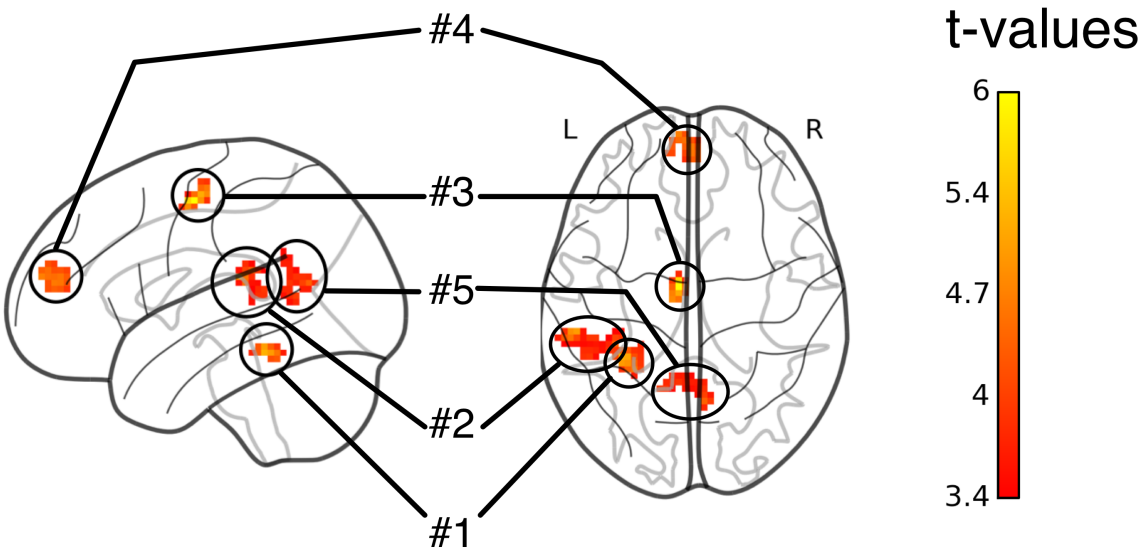

Figure 5

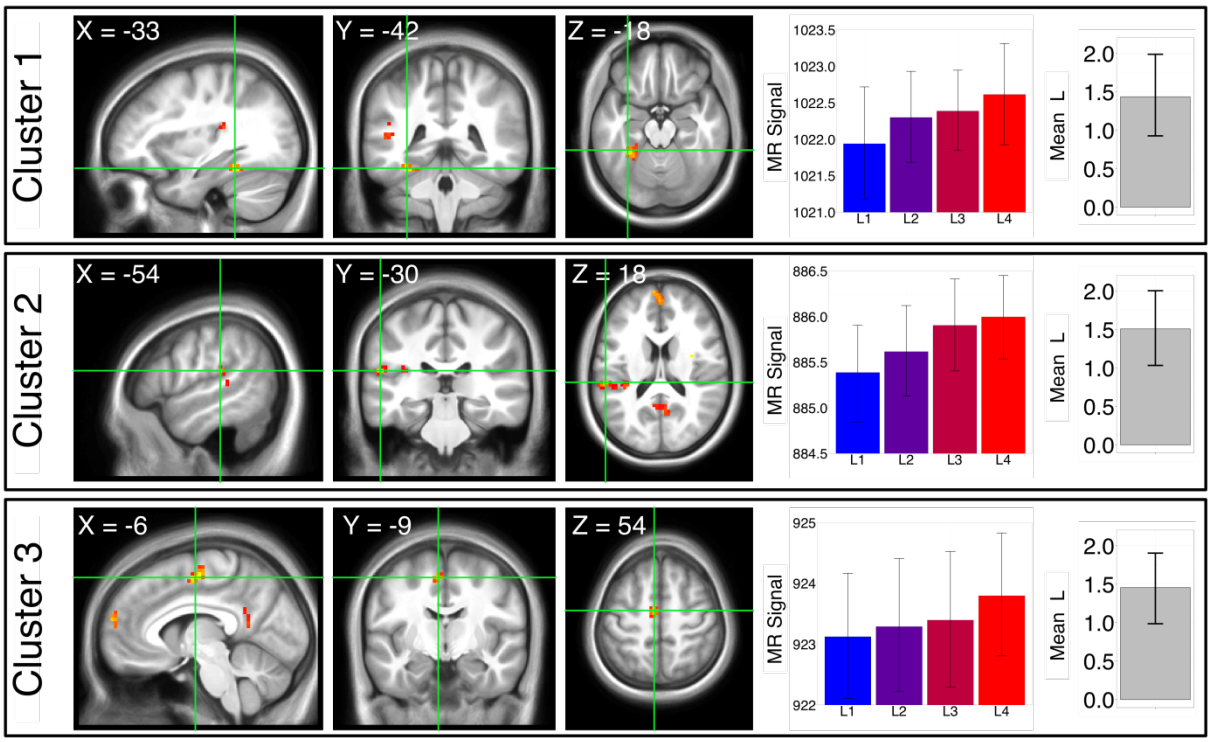
Cluster 1
X = -33
Y = -42
Z = -18
MR Signal
1023.5
1023.0
1022.5
1022.0
1021.5
1021.0
L1
L2
L3
L4
Mean L
2.0
1.5
1.0
0.5
0.0
Cluster 2
X = -54
Y = -30
Z = 18
MR Signal
886.5
886.0
885.5
885.0
884.5
L1
L2
L3
L4
Mean L
2.0
1.5
1.0
0.5
0.0
Cluster 3
X = -6
Y = -9
Z = 54
MR Signal
925
924
923
922
L1
L2
L3
L4
Mean L
2.0
1.5
1.0
0.5
0.0

Figure 6